# Forward $K_S^0K_S^0$ production in 200-GeV/$c$ $\pi^-N$ interactions

E. G. H. Williams, J. M. Marraffino, C. E. Roos, J. W. Waters, and M. S. Webster
*Vanderbilt University, Nashville, Tennessee 37235*

R. N. Diamond,* C. C. Chang, T. C. Davis, K. J. Johnson,† R. W. Joyner, and J. A. Poirier
*University of Notre Dame, Notre Dame, Indiana 46556*

A. Napier and J. Schneps
*Tufts University, Medford, Massachusetts 02155*

T. Y. Chen,‡ E. W. Jenkins, K. W. Lai, J. LeBritton,§ Y. C. Lin,** and A. E. Pifer
*University of Arizona, Tucson, Arizona 85721*

H. C. Fenker and D. R. Green
*Fermilab, Batavia, Illinois 60510*

J. R. Albright, J. H. Goldman, S. L. Hagopian, J. E. Lannutti, and J. E. Piper
*Florida State University, Tallahassee, Florida 32306*

J. R. Ficenec and W. P. Trower
*Virginia Polytechnic Institute and State University, Blacksburg, Virginia 24061*
(Received 19 March 1984; revised manuscript received 15 June 1984)

Forward $K_S^0K_S^0$ production ($x_F>0.2$) with an associated charged multiplicity of five or less has been observed in an experiment designed to trigger on two neutral strange particles. The $K_S^0K_S^0$ mass distribution shows $f^0(1270)$, $A_2(1320)$, $f'(1515)$, and $S^{*\prime}(1730)$ production with cross sections/nucleon for $x_F>0.2$ of $49\pm17$, $54\pm15$, $1.4\pm0.4$, and $0.6\pm0.2$ $\mu$b, respectively. The differential cross sections indicate central production of the $S^*(975)$, whereas the $f^0(1270)$, $A_2(1320)$, $f'(1515)$, and $S^{*\prime}(1730)$ have a sizable leading component. Inclusive $K_S^0$ production in this data sample is described by a $(1-x_F)^{1.6}$ distribution in qualitative agreement with simple quark-counting rules. Both the $K_S^0K_S^0$ and single-$K_S^0$ $p_T{}^2$ distributions at large $x_F$ show evidence for diffractive or resonance production.

New states have been most readily observed in formation and production processes when restrictions exist on the quantum numbers of the initial- or final-state particles. The $J/\psi$ (Refs. 1,2) and $\Upsilon$ (Ref. 3) states are the most prominent recent examples of this situation. The goal of the present experiment was to look for new states of definite $J^P$ decaying to two neutral strange particles, specifically $K\bar{K}$ and $\Lambda\bar{\Lambda}$. The $\Lambda\bar{\Lambda}$, as well as $K_S^0\Lambda$, $K_S^0\bar{\Lambda}$, $K_S^0K_S^0\pi^-$, and $K_S^0K_S^0\pi^+\pi^-\pi^-$ data samples are discussed in other papers.[4–8] We consider here the $K_S^0K_S^0$ events, which have $J^P$ restricted to $0^+$, $2^+$, $4^+$, etc.

The experiment (E-580) was carried out in the Fermilab multiparticle spectrometer (MPS) with a 200-GeV/$c$ $\pi^-$ beam. The target consisted of 20 layers of 0.25-in. plastic scintillator and was followed by a 2.14-m helium-filled decay region located 0.73 m downstream of the active target. The superconducting spectrometer magnet imparted a 697-MeV/$c$ transverse-momentum kick to the charged tracks. Event reconstruction was made possible by a chamber system with 10 000 proportional wires and 24 planes of magnetostrictive spark chambers. The experiment was designed to trigger on the production of two neutral strange particles by counting hits in two proportional-wire-chamber (PWC) planes located between the target and decay region and in seven downstream PWC planes, four immediately following the decay region and three after the magnet. An increase of four ($\pm$ one) in the multiplicity was required by the trigger. An additional requirement was made that the number of directly produced charged particles through the spectrometer be five or fewer. More details on the experimental setup are contained in Refs. 6 and 8.

Approximately $1.2\times10^6$ triggers were processed through pattern recognition, geometry, and kinematics programs and yielded $70.5\times10^3$ two-$V^0$ events. These two-$V^0$ events were composed of 62% $K_S^0K_S^0$, 8% $\Lambda\bar{\Lambda}$, 29% $K_S^0\Lambda$ or $K_S^0\bar{\Lambda}$, and 1% $\Lambda\Lambda$ or $\bar{\Lambda}\bar{\Lambda}$. The $\Lambda$ or $\bar{\Lambda}$ contamination in the $K_S^0K_S^0$ data sample is estimated to be 2%. At a typical momentum of 29 GeV/$c$ the unfitted $K_S^0$ mass resolution is estimated to be 14 MeV full width at half maximum (FWHM). The $K_S^0K_S^0$ mass resolution at a momentum of 40 GeV/$c$ varies from 25 MeV at a mass of 1.9 GeV to 55 MeV at a mass of 3.5 GeV based on studies of the $K_S^0$, $\Lambda$, $K^{*+-}(890)$, $K^{*+-}(1420)$, $\Sigma^{+-}(1380)$, and $\Xi^-(1320)$.

The MPS was configured to optimize the combined

 

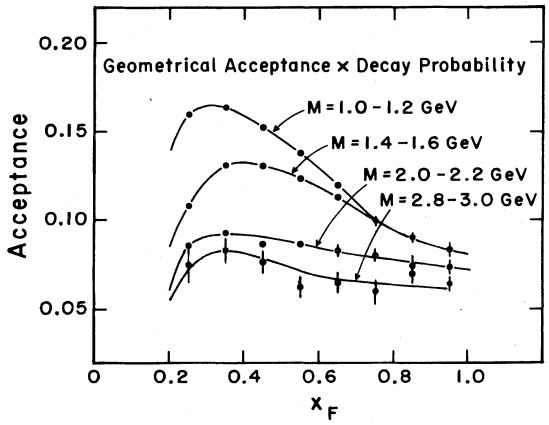


FIG. 1. Geometric acceptance times decay probability as a function of $x_F$ for various ranges of effective $K_S^0K_S^0$ mass. The acceptance is calculated for our $K_S^0K_S^0$ data on an event-by-event basis as described in the text. The curves are merely guides for the eye.

geometrical acceptance (typically 70—85% for $K_S^0K_S^0$ masses of 2 GeV) for particles produced forward in the center-of-mass ($x_F > 0.2$) and probability (15%) for both decays to occur within the decay region. Figure 1 shows the combined geometrical acceptance and decay probability as a function of $x_F$ for various values of $K_S^0K_S^0$ mass. Because of inefficiencies and clustering in the PWC's used in the trigger, the trigger efficiency was dependent upon the associated charged particle multiplicity. For the trigger-efficiency calculation chamber efficiencies were obtained using diagnostic triggers containing noninteracting beam tracks.

The data discussed in this paper contain 27 136 $K_S^0K_S^0$ events which satisfy the fiducial-volume and track-quality cuts described in Ref. 6. The effective-mass distribution of the $K_S^0K_S^0$ events is shown in Fig. 2. There is clear evi-

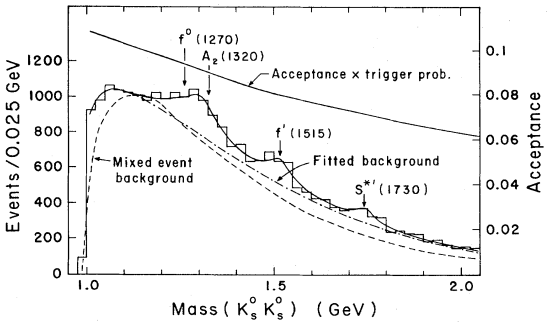


FIG. 2. $K_S^0K_S^0$ mass distribution. The solid curve is the result of a fit to the data using the background function (dashed-dotted curve) and known resonance parameters for the $f^0$ (1270), $A_2$ (1320), and $f'$ (1515). The fitted mass and width of the $S^{*\prime}$ (1730) where $M = 1.742 \pm 0.015$ GeV, $\Gamma = 0.057 \pm 0.038$ GeV. A curve for the combined decay probability and geometric acceptance times trigger efficiency as a function of mass is also shown. A dashed curve representing the background based on mixed events which do not violate energy-momentum conservation is included.

dence close to threshold for structure in the mass plot. The accepted values of the $f^0(1270)$, $A_2(1320)$, and $f'(1515)$, are indicated in the figure. The $S^{*\prime}(1730)$, which has been seen in only one other experiment,[9] also appears in the figure. Above the $f'(1515)$ the only evidence for structure in the $K_S^0K_S^0$ mass spectrum is in the region of the $S^{*\prime}(1730)$.

The solid curve in Fig. 2 was obtained by fitting the mass spectrum to a background shape (dashed-dotted curve) plus incoherent sum of Breit-Wigner resonance forms for the $f^0(1270)$, $A_2(1320)$, $f'(1515)$, and $S^{*\prime}(1730)$. The proximity of the $f^0(1270)$ and $A_2(1320)$ to each other, their widths, and the experimental mass resolution make a clear separation of these resonances ambiguous. We have nevertheless chosen to parametrize the $K_S^0K_S^0$ mass spectrum this way rather than by a single peak of arbitrary shape and width in the $f^0(1270)/A_2(1320)$ mass region. The $\chi^2$/DF for the fit is 0.95. The mass and width for all resonances except the $S^{*\prime}$ were fixed at values given by the Particle Data Group.[10] The fitted $S^{*\prime}$ parameters are $M = 1.742 \pm 0.015$ GeV and $\Gamma = 0.057 \pm 0.038$ GeV. The background curve has the form

$$(M - M_{\text{th}})^{\alpha} \exp(-\beta M - \gamma M^2) , \tag{1}$$

where $M$ is the $K_S^0K_S^0$ mass, $M_{\text{th}}$ is the threshold mass, and $\alpha$, $\beta$, $\gamma$ are parameters to be determined.

The acceptance curve plotted in Fig. 2 indicates that the combined decay probability times geometrical acceptance times trigger probability decreases smoothly over the mass range from 1—2 GeV at a rate much less than the falloff in the mass spectrum. The decay probability was obtained for each $K_S^0$ using its potential decay length and momentum. The geometric acceptance was obtained by generating for each real event 100 events rotated about the beam direction, letting each $K_S^0$ decay isotropically in its rest frame at random locations in the decay volume consistent with its lifetime, and tracing each decay product through the magnet and chambers which constitute the MPS. The trigger efficiency, which depends on the number of primary tracks accompanying the two vees, was calculated from the efficiencies of the chambers used in the hardware trigger. An additional factor, the software reconstruction efficiency, was obtained using a subset of the real data to produce hits in each chamber according to its known efficiency, smearing the coordinates by taking into account each chamber's wire spacing, and generating a pseudodata record for each event. The resulting Monte Carlo output was processed through the same analysis programs as the real data in order to obtain the reconstruction efficiency.

Combining the geometrical acceptance and decay probability with the trigger efficiency and software reconstruction efficiency we obtain an average sensitivity for this experiment for forwardly produced $K_S^0K_S^0$ pairs ($x_F > 0.2$) of $1470 \pm 340$ events/$\mu$b, based on an effective incident beam of $1.0 \times 10^{10}$ pions and a scintillator (CH) target of 15.58 g/cm$^2$. This corresponds to a forward $K_S^0K_S^0$ cross section of $16.2 \pm 3.8$ $\mu$b per nucleon assuming an $A^1$ dependence. The trigger efficiency is a sensitive function of chamber efficiency and due to varying operating condi-

tions we estimate the uncertainty in the trigger efficiency at 20%. This is the largest contribution to the error in the sensitivity.

As a check on our sensitivity calculation a sample of $K_S^0K_S^0$ events from the Fermilab 15-ft hydrogen-filled bubble chamber has been processed through an acceptance program similar to that described above. It was found, with poor statistics, that of the $620\pm200$ $\mu$b inclusive cross section[11] only $19\pm9$ $\mu$b (Ref. 12) would be accepted by our experiment. Thus our cross-section normalization is in good agreement with that expected from the bubble chamber.

The average sensitivity of the experiment can be calculated in a number of ways. In this paper, the sensitivity used for the differential cross sections is based on the number of effective (dead-time-corrected) beam tracks, target thickness, and estimates of the various acceptances in the experiment on an event-by-event basis as described above. The average value of $1470\pm340$ events/$\mu$b nucleon quoted here is for $K_S^0K_S^0$ events with $x_F>0.2$ and associated charged multiplicity $\leq 5$.

Our previously published data have relied on two other approaches to relate our observations to inclusive $K_S^0K_S^0$ production as measured in the bubble chamber.

The first approach, similar to that employed in our inclusive $K_S^0\Lambda$ paper,[4] was to divide the total $K_S^0K_S^0$ cross section[11] of $620\pm200$ $\mu$b into the observed number of $K_S^0K_S^0$ events and yields for our data a normalization factor of $44\pm14$ events/$\mu$b. This normalization factor implies that our estimated total cross sections will be roughly 33 times the directly measured cross sections with $x_F>0.2$ and associated charged multiplicity $\leq 5$. We will make use of this approach in this paper when we calculate the total cross sections for the production of the resonances seen in Fig. 2.

The second approach, employed in our studies of diffractive $K_S^0K_S^0$ production, used an $\exp(-6x_F)$ distribution for $d\sigma/dx_F$ of the $K_S^0K_S^0$ pair. This distribution, based on bubble-chamber results, was convoluted with our acceptance to yield a sensitivity of $450\pm150$ events/$\mu$b for $K_S^0K_S^0\pi^-$ and $240\pm80$ events/$\mu$b for $K_s^0K_S^0\pi^+\pi^-\pi^-$ in Refs. 6 and 7, respectively. The $x_F$ distribution used in the extrapolation was determined from bubble-chamber data for which the bulk of the data[12] has $x_F<0.2$. As we now show, this bubble-chamber $x_F$ distribution falls more rapidly than does our data.

The $x_F$ distribution for inclusive $K_S^0K_S^0$ production is displayed in Fig. 3(a), while the invariant differential cross section is presented in Fig. 3(b). A simple exponential has been fitted to the distribution in Fig. 3(a) over the region $0.4\leq x_F\leq 0.9$ and yields a slope parameter of $3.2\pm0.1$. This slope is a factor of 2 shallower than that seen in the bubble chamber and leads to a factor-of-2 increase in the sensitivity quoted in our previously published papers on diffractive production. The invariant cross section in Fig. 3(b) shows evidence of diffractive or resonance production for $x_F>0.8$. This observation is consistent with the fact that most of the events in this region have an associated charged multiplicity $\leq 1$.

In Fig. 4, we plot the differential cross section $d\sigma/dp_T{}^2$ for inclusive $K_S^0K_S^0$ production. This distribution has been fitted with a simple exponential and is well described by an $\exp(-bp_T{}^2)$ distribution, with $b=2.1\pm0.1$ $(\mathrm{GeV}/c)^{-2}$. This $p_T{}^2$ slope is shallower than the bubble-chamber result[12] which is primarily for $x_F<0.2$. The $p_T{}^2$ distributions are shown in Fig. 4 for events corresponding to various $x_F$ regions. The slope appears to remain fairly constant, in contrast to single-particle results.[13] At high $x_F$ ($x_F>0.7$) we do seem to see a steeper slope. If we parametrize the data by a sum of two exponentials, the shallower slope has essentially the same value of 2.1 $(\mathrm{GeV}/c)^{-2}$ as the bulk of the data. The steeper com-

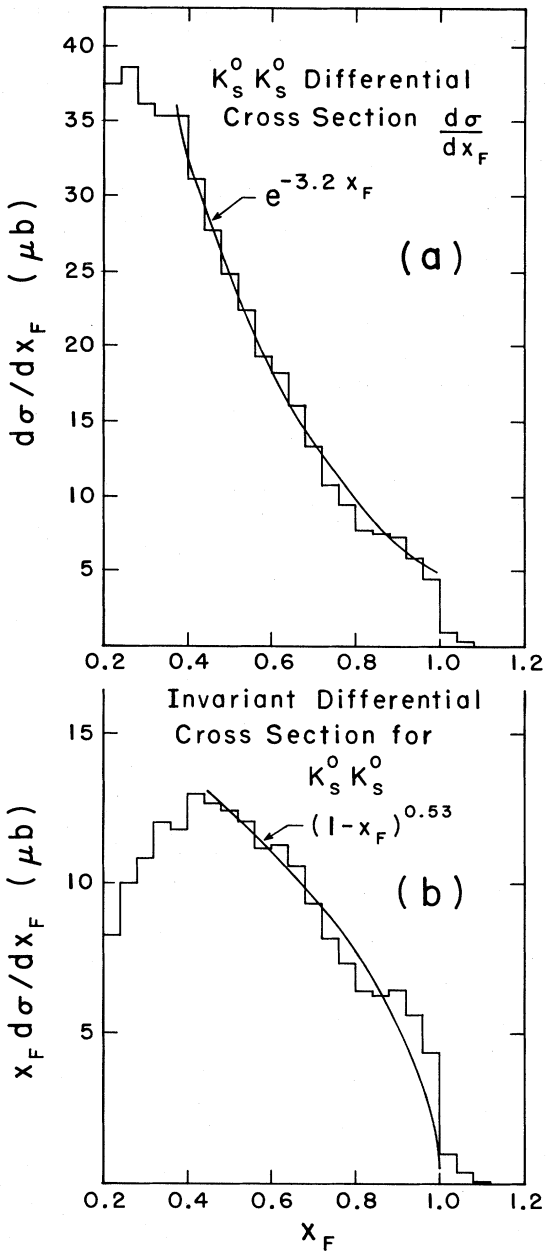


FIG. 3. (a) The measured $K_S^0K_S^0$ cross section $d\sigma/dx_F$, corrected for acceptance and trigger efficiency. (b) The $K_S^0K_S^0$ invariant cross section $(x_F)(d\sigma/dx_F)$ for $x_F>0.2$.

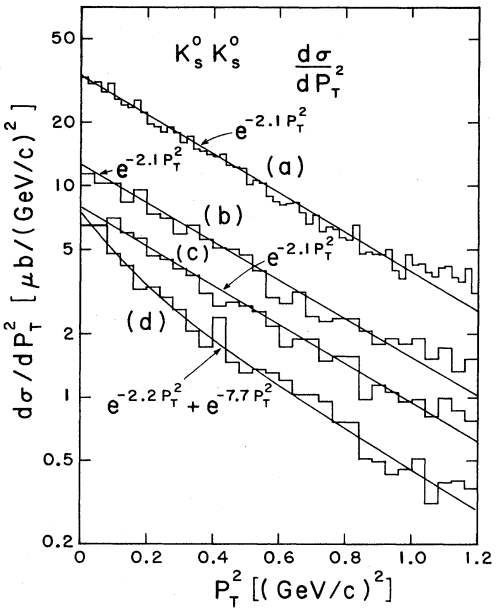


FIG. 4. The inclusive $K_S^0K_S^0$ $p_T{}^2$ distribution, $d\sigma/dp_T{}^2$. The distributions shown correspond to (a) all events with $K_S^0K_S^0$ $x_F>0.2$, (b) events with $0.3<x_F<0.5$, (c) events with $0.5<x_F<0.7$, and (d) events with $0.7<x_F<1.0$.

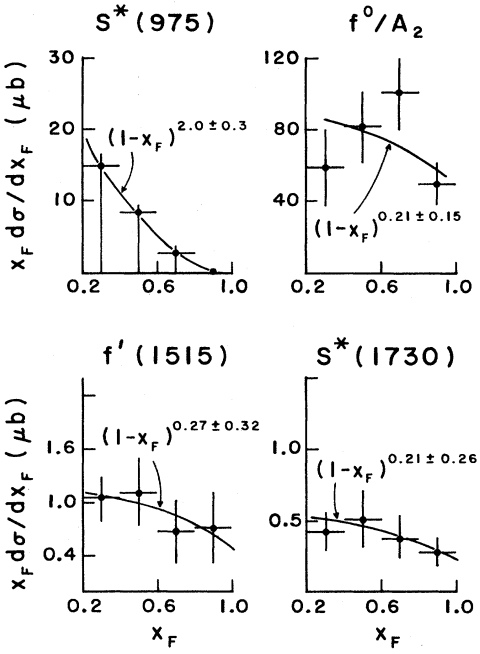


FIG. 5. The invariant $x_F$ distributions for the resonances found in Fig. 2. The curves are fits of the form $(1-x_F)^\alpha$.

ponent may be associated with diffractive production.

Table I shows the observed number of events, $K\bar{K}$ branching ratio, and two cross sections for each of the resonances seen in Fig. 2. The $S^*{}'(1730)$ has been seen only in the $K_S^0K_S^0$ decay mode,[9] and we have therefore taken the $K\bar{K}$ decay mode to have a 100% branching fraction. The first cross section, measured directly in this experiment, is for $K_S^0K_S^0$ events with $x_F>0.2$ and with five or fewer accompanying charged pions and is corrected for the decay branching fraction. The total cross section estimates for the resonances are calculated using the normalization factor of $44\pm14$ events/$\mu$b, the decay branching fraction, and the relative acceptance at the resonance mass.

Table I also contains two entries for the $S^*(975)$. Using the functional form of Eq. (1) to represent the background in the $K_S^0K_S^0$ mass spectrum of Fig. 2, we find little evidence for the $S^*(975)$. However, the background shape near $K_S^0K_S^0$ threshold is not well understood. A plausible background shape can be obtained by combining kaons from different events which have the same multiplicity and which also do not violate energy-momentum conservation. In addition to the actual observed (raw) number of $S^*(975)$ events obtained by subtracting the mixed-event $K_S^0K_S^0$ background, a corrected number was obtained under the assumption that the $S^*$ could be represented by a Breit-Wigner shape with mass 975 MeV and total width 40 MeV. Integrating the distribution from threshold to 1150 MeV gives a correction factor of 4.5. A partial-wave analysis of $K^+K^-$ at threshold indi-

TABLE I. Parameters and cross sections for the resonances found in the $K_S^0K_S^0$ mass spectrum. The number of observed events with associated charged multiplicity $\leq 5$, the corresponding cross section for $x_F>0.2$, and extrapolated total cross section for each resonance are given.

| Resonance | Observed no. of events | $K\bar{K}$ branching ratio | Cross section[a] ($n_c\leq5$, $x_F>0.2$) ($\mu$b) | Total cross section[b] ($\mu$b) |
|---|---|---|---|---|
| $S^*(975)$[c] | $585^{+65}_{-585}$ (raw) | 0.22 | $5.7^{+1.5}_{-5.7}$ | $190^{+50}_{-190}$ |
| | $2630^{+300}_{-2630}$ (corrected) | 0.22 | $26^{+7}_{-26}$ | $860^{+220}_{-860}$ |
| $f^0(1270)$ | 580±150 | 0.029 | 49±17 | 1630±670 |
| $A_2(1320)$ | 1050±170 | 0.048 | 54±15 | 1800±740 |
| $f'(1515)$ | 520±90 | 1.00 | 1.4±0.4 | 47±17 |
| $S^*{}'(1730)$[d] | 200±60 | 1.00 | 0.60±0.22 | 20±8 |

[a]Based on forward sensitivity of 1470±340 events/$\mu$b with associated charged multiplicity $\leq5$.
[b]Based on average normalization of 44±14 events/$\mu$b.
[c]Using mixed events for background estimate.
[d]Fitted values: $M(S^*{}')=1.742\pm0.015$ GeV. $\Gamma(S^*{}')=0.057\pm0.038$ GeV.

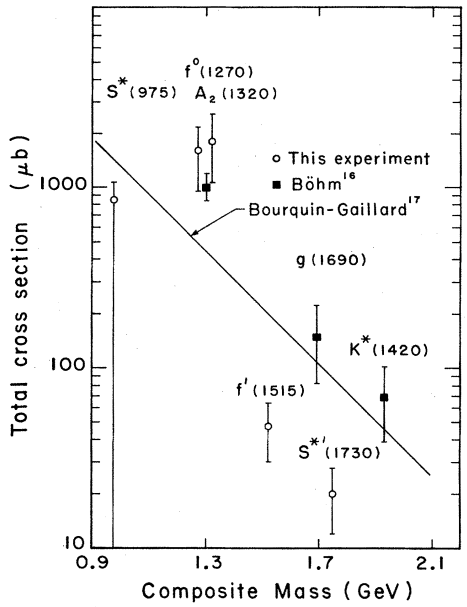


FIG. 6. Production cross sections for $S^*$, $f$, $A_2$, $f'$, and $S^{*\prime}$ at 200 GeV/$c$ compared with ISR data (Ref. 16) and with the Bourquin-Gaillard model (Ref. 17).

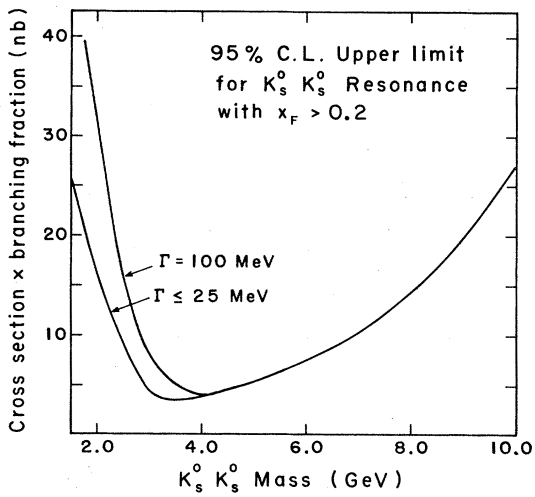


FIG. 7. Upper limits (95% confidence level) for the production of a resonance decaying to $K_S^0K_S^0$, with $x_F > 0.2$ and associated charged multiplicity $\leq 5$.

cates that the $S^*$ is a virtual $K\bar{K}$ bound state with a width below $K\bar{K}$ threshold of 40 MeV.[14] Some theoretical speculations[15] suggest that it is a centrally produced four-quark state.

The invariant $x_F$ distribution for the resonances in Table I have been extracted from the data in each $x_F$ interval using techniques similar to those described above but with all resonance parameters fixed. The invariant differential cross sections corrected for acceptance and trigger efficiency are plotted in Fig. 5. The data have been fit to the form $(1-x_F)^\alpha$. As can be seen in the figure, the $S^*(975)$ is produced predominantly in the low $x_F$ or central region and has a $(1-x_F)^{2.0\pm0.3}$ distribution. The invariant $x_F$ distributions of the $f^0(1270)$ and $A_2(1320)$ have been combined. Along with the $f'(1515)$ and $S^{*\prime}(1730)$, the $f^0/A_2$ has been fit to $(1-x_F)^\alpha$. All three distributions are consistent with $\alpha=0.23\pm0.25$ and indicate a significant leading-particle component.

These resonance total cross sections are plotted in Fig. 6 along with entries for the $f^0$, $g$, and $K^*(1420)$ mesons from a CERN ISR experiment[16] and for the $\rho^0$ from a Fermilab bubble-chamber experiment.[17] The curve in Fig. 6 is calculated from the Bourquin-Gaillard model,[18] which estimates the inclusive cross sections for resonance production as a function of the resonance mass. The ISR production cross sections for $f^0$, $g$, and $K^*(1420)$ have been extrapolated to our energy region using the Bourquin-Gaillard energy dependence. The $K^*(1420)$ appears at a mass of 1920 MeV due to the composite mass scale inherent in the model. In this model each unit of strangeness in the resonance requires the composite mass to be increased by 500 MeV because an additional strange quark must be pulled from the sea.

A goal of this experiment was to search for new resonances decaying to $K_S^0K_S^0$. We present in Fig. 7 the upper limits for the cross section times branching fraction as functions of $K_S^0K_S^0$ mass for the production of such resonances with $x_F > 0.2$. The two curves relate to different assumptions about the resonance: the lower curve corresponds to a resonance whose assumed width of 25 MeV is narrower than our mass resolution which dominates the upper-limit calculation; the upper curve to a resonance whose width of 100 MeV is much wider than our resolution. The upper limit decreases because the background falls more steeply than does the sensitivity of the experiment. Beyond a $K_S^0K_S^0$ mass of 4 GeV, the background is negligible and the upper limit rises as the sensitivity continues to decrease. At the 95% confidence level a narrow resonance with a mass of 2 GeV and a cross section times branching fraction of $16\pm3.8$ nb would be observed in this experiment. These curves do not reflect the uncertainty in our experimental sensitivity of 23% which should be added in quadrature.

We turn now to the single $K_S^0$ distributions, which can be obtained from this $K_S^0K_S^0$ data sample. To the extent that associated production can be neglected, these distributions can be compared with inclusive data from other experiments. In Fig. 8(a) we plot the $K_S^0$ $x_F$ distribution and in Fig. 8(b) the invariant cross section $x_Fd\sigma/dx_F$. One curve in Fig. 8(b) is a fit over the interval $0.2<x_F<0.8$ to a distribution of the form $(1-x_F)^\alpha$ with $\alpha=1.61\pm0.03$. This value for $\alpha$ is consistent with the Fermilab single-arm spectrometer (SAS) results.[13] Simple quark-counting rules[19] in which the $K_S^0$ is both $K^0$ and $\bar{K}^0$, predict that the $x_F$ distribution is a linear combination of $(1-x_F)^3$ and $(1-x_F)^1$. The other curve is a fit to the form $A(1-x)^3+B(1-x)^1$ which yields $A/B=1.54\pm0.09$.

The $p_T^2$ distribution shown in Fig. 9 for $K_S^0$ is described by a sum of two exponentials with slopes $2.3\pm0.1$ and $5.2\pm0.2$ $(\text{GeV}/c)^{-2}$. The shallower slope parameter is in reasonable agreement with the SAS results

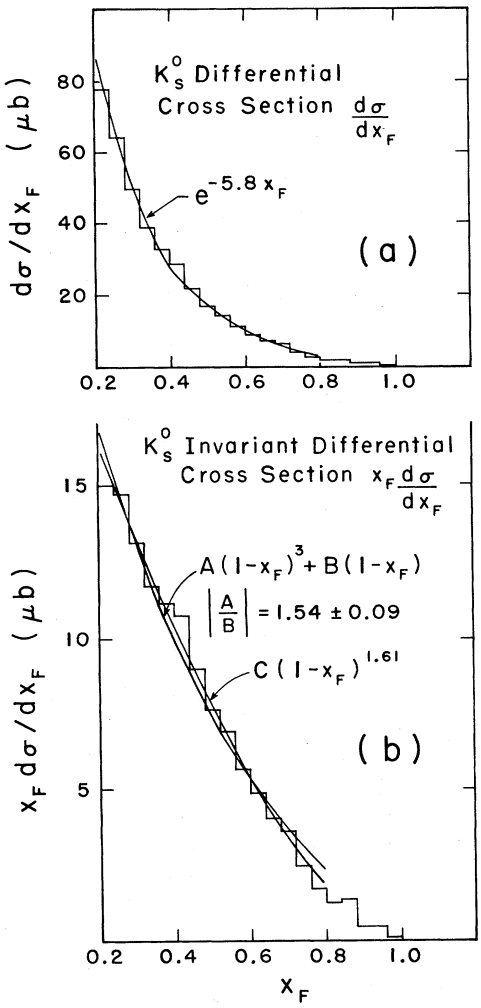


FIG. 8. (a) The $K_S^0$ $x_F$ distribution for $K_S^0$ produced in association with another $K_S^0$. (b) The $K_S^0$ invariant $x_F$ distribution $x_F\, d\sigma/dx_F$ for $K_S^0$ produced in association with another $K_S^0$. The curves are a $(1-x_F)^{1.6\pm0.03}$ function normalized to the data and a sum of $(1-x_F)^3$ plus $(1-x_F)^1$.

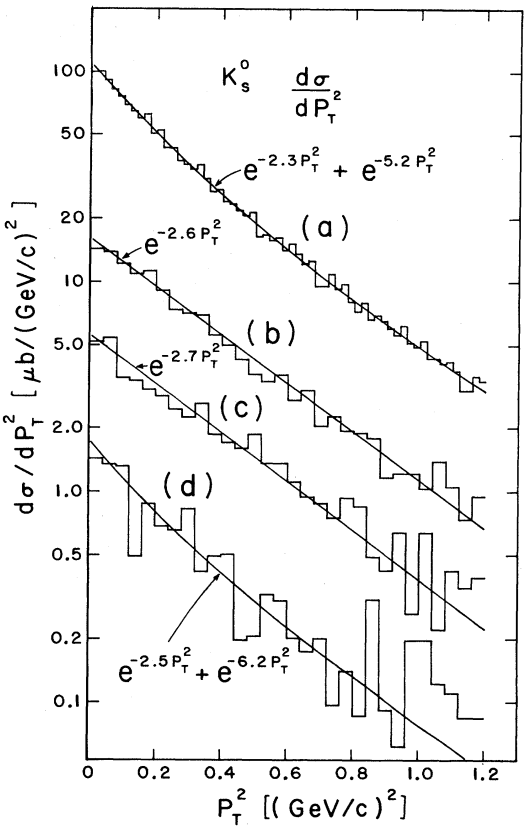


FIG. 9. The $K_S^0$ $p_T{}^2$ distribution of $K_S^0$ produced in association with another $K_S^0$ for which $x_F$ of the pair is greater than 0.2. The distributions shown correspond to (a) all events with single $K_S^0$ $x_F > 0$, (b) events with $0.3 < x_F < 0.5$, (c) events with $0.5 < x_F < 0.7$, and (d) events with $0.7 < x_F < 1.0$.

and is also consistent with most hadronic $p_T{}^2$ distributions. In Fig. 9, we also show the $p_T{}^2$ distribution for various slices in $x_F$ of the $K_S^0$. We note a slightly steeper $p_T{}^2$ slope as $x_F$ increases, an effect also seen in the SAS results. We note that the $K_S^0$ $p_T{}^2$ distribution has a more rapid falloff than does the same distribution for $K_S^0K_S^0$. This effect is expected from uncorrelated $K_S^0K_S^0$ combinations. At large $x_F$, we also note an enhancement at low $p_T{}^2$, which may be associated with diffractive processes or resonance production. Fitting the data to a sum of two exponentials, as done for the $K_S^0K_S^0$ distribution, we find that the shallower term has the same slope as the bulk of the data.

The results of this experiment on $K_S^0K_S^0$ production can be summarized as being generally consistent with other hadroproduction experiments despite our limited acceptance and restrictions on associated charged multiplicity. We observe the $S^*(975)$, $f^0(1270)/A_2(1320)$, $f'(1515)$, and $S^{*\prime}(1730)$, but no higher mass resonances. The invariant $x_F$ distributions show the $S^*(975)$ to be centrally produced, while the other resonances have a significant leading-particle component. The single-$K_S^0$ distributions in these data are also consistent with other experiments.

## ACKNOWLEDGMENTS

We wish to thank the Fermilab staff, especially S. Hansen and R. Cantel for their valuable help during the experiment. This work was supported in part by Department of Energy contracts (Arizona, Florida State, and Tufts) and National Science Foundation grants (Arizona, Notre Dame, Vanderbilt, and Virginia Tech.).

*Former address: Florida State University, Tallahassee, Florida 32306.
†Present address: Motorola Inc., Phoenix, Arizona 85008.
‡Present address: Dept. of Physics, Nanking University, Nanking, People's Republic of China.
§Present address: Burr-Brown Research Corp., Tucson, Arizona 85706.
**Present address: 1782 Calle Yucca, Thousand Oaks, California 91360.

[1]J. J. Aubert *et al.*, Phys. Rev. Lett. 33, 1404 (1974).

[2]J. E. Augustin *et al.*, Phys. Rev. Lett. **33**, 1406 (1974).
[3]S. W. Herb *et al.*, Phys. Rev. Lett. **39**, 252 (1977).
[4]H. C. Fenker *et al.*, Phys. Rev. D **30**, 872 (1984).
[5]J. Ficenec *et al.* (unpublished).
[6]T. Y. Chen *et al.*, Phys. Rev. D **28**, 2304 (1983).
[7]C. C. Chang *et al.*, Phys. Rev. D **29**, 1888 (1984).
[8]J. Poirier *et al.*, in *Multiparticle Dynamics 1981,* Proceedings of the XIIth International Symposium, Notre Dame, Indiana, edited by W. D. Shephard and V. P. Kenney (World Scientific, Singapore, 1982), p. 153.
[9]A. Etkin *et al.*, Phys. Rev. D **25**, 2446 (1982).
[10]Particle Data Group, Phys. Lett. **111B**, 1 (1982).
[11]D. Bogert *et al.*, Phys. Rev. D **16**, 2098 (1977).
[12]S. Hagopian (unpublished). See Ref. 11.
[13]A. E. Brenner *et al.*, Phys. Rev. D **26**, 1497 (1982).
[14]A. B. Wicklund *et al.*, Phys. Rev. Lett. **45**, 1469 (1980).
[15]R. J. Jaffe, Phys. Rev. D **15**, 267 (1977).
[16]A. Böhm *et al.*, Phys. Rev. Lett. **41**, 1761 (1978).
[17]F. C. Winkelman *et al.*, Phys. Lett. **56B**, 101 (1975).
[18]M. Bourquin and J. M. Gaillard, Nucl. Phys. B **114**, 334 (1976).
[19]J. F. Gunion, in *Proceedings of the XVth Rencontre de Moriond, Les Arcs, Savoie, France, 1980,* edited by J. Tran Thanh Van (Editions Frontières, Dreux, France, 1980), Vol. 1, p. 151; Phys. Lett. **88B**, 150 (1979).